

Leakage Current Reduction of Ni-MILC Poly-Si TFT Using Chemical Cleaning Method

Kwang-Jin Lee¹, Doyeon Kim², Duck-Kyun Choi^{1†} and Woo-Byoung Kim^{2†}

¹Department of Materials Science & Engineering, Hanyang University, Seoul 04763, Republic of Korea

²Department of Energy Engineering, Dankook University, Cheonan 31116, Republic of Korea

(Received May 14, 2018 : Revised July 9, 2018 : Accepted July 21, 2018)

Abstract An effective cleaning method for Ni removal in Ni-induced lateral crystallization(Ni-MILC) poly-Si TFTs and their electrical properties are investigated. The HCN cleaning method is effective for removal of Ni on the crystallized Si surface, while the nitric acid treatment results decrease by almost two orders of magnitude in the Ni concentration due to effective removal of diffused Ni mainly in the poly-Si grain boundary regions. Using the HCN cleaning method after the nitric acid treatment, re-adsorbed Ni on the Si surfaces is effectively removed by the formation of Ni-cyanide complexes. After the cleaning process, important electrical properties are improved, e.g., the leakage current density from 9.43×10^{-12} to 3.43×10^{-12} A and the subthreshold swing values from 1.37 to 0.67 mV/dec.

Key words nickel removal, poly-Si TFTs, nitric acid treatment, hydrogen cyanide cleaning.

1. Introduction

Low temperature crystallization methods are considered to be an essential method to achieve high mobility for poly-crystalline silicon(poly-Si) thin film transistors(TFTs).¹⁻²⁾ Many researchers have been focused on the laser-based crystallization methods(e.g., excimer-laser crystallization(ELC)).³⁻⁵⁾ Although there are many advantages in the ELC technology and its derivatives, a limit of incident laser beam length⁶⁾ and high surface roughness(i.e., ridge structure formed by laser annealing) hinder the future application in large scale displays. High process cost of the laser crystallization technique is another concern. On the other hand, non-laser low temperature crystallization methods using metal catalyst[e.g., metal-induced crystallization(MIC),⁷⁾ metal-induced lateral crystallization(MILC),⁸⁾ field-aided lateral crystallization(FALC),⁹⁾ etc.] have demonstrated themselves as potential cost effective methods for large scale displays compared to the laser-based crystallization methods. However, residual metal contaminants (typically Ni and its compound NiSi₂) after the crystallization process on the surface and/or inside of crystallized Si bulk deteriorate the major electrical properties and

result in high off-state leakage current, a shift in threshold voltage(V_{th}), subthreshold swing, etc.¹⁰⁾

Cleaning employed in electronic device fabrication processes is usually performed with the RCA method which uses mixtures of H₂O₂ plus NH₄OH solutions(i.e., SC1 cleaning), and H₂O₂ plus HCl solutions(i.e., SC2 cleaning), but is mostly accompanied by surface etching and re-adsorption of removed metal contaminants. Recently, H. Kobayashi and colleagues have reported a simple metal removal method on Si surfaces using cyanide solutions[i.e., potassium cyanide(KCN) and hydrogen cyanide(HCN)], that can avoid the etching problem.¹¹⁻¹³⁾ This method shows effective removal of metal contaminants to the concentration less than 3×10^9 atoms/cm². Extremely low concentration cyanide solutions(e.g., 3 ppm) can be used for cleaning. Moreover, re-adsorption of metal contaminants does not occur,¹²⁾ which enables repeated use of the cleaning solutions. Moreover, using two kinds of chemical solutions, e.g., HCl + H₂O₂ and HCN solutions, metal contaminants on SiC surfaces can completely be removed in spite of the fact that SiC is much more chemically stable, and thus the RCA cleaning method is not effective.¹⁴⁾ It should be noted that defect states near

[†]Corresponding authors

E-Mail : woo7838@dankook.ac.kr (W.-B. Kim, Dankook Univ.)

duck@hanyang.ac.kr (D.-K. Choi, Hanyang Univ.)

© Materials Research Society of Korea, All rights reserved.

This is an Open-Access article distributed under the terms of the Creative Commons Attribution Non-Commercial License (<http://creativecommons.org/licenses/by-nc/3.0>) which permits unrestricted non-commercial use, distribution, and reproduction in any medium, provided the original work is properly cited.

Si and SiC surfaces are simultaneously passivated because cyanide ions (CN^-) in the solutions are directly and selectively adsorbed on the defect sites, leading to formation of Si-CN bonds. Si-CN bonds are thermally stable up to 800 °C because of their high bond energy of 4.5 eV¹⁵ (cf. Si-H bond energy: 3.1~3.5 eV¹⁶⁻¹⁷).

The aim of the present study is to find the effective way of eliminating Ni in the crystallized poly-Si using the CN-based chemical cleaning method after the Ni-MILC process and to investigate the cleaning effect on the electrical properties of TFTs.

2. Experiments

Ni-MILC top gate poly-Si TFT samples were prepared by following processes. Firstly, 300 nm thick SiO_2 was deposited on a Corning 1737 glass substrate using atmospheric pressure chemical vapor deposition (APCVD) at 300 °C. Then, a 50 nm thick amorphous Si layer was deposited at 400 °C by a low pressure chemical vapor deposition (LPCVD) method using SiH_4 gas. In order to form active regions and transistor gate regions, photolithography and patterning methods were used. Ni-induced lateral crystallization (Ni-MILC) of the active regions was carried out by selective deposition of a 2 nm thick Ni catalyst layer on the source and drain areas by a DC sputtering method, followed by the heat treatment at 500 °C for 10 h in nitrogen atmosphere.

Chemical solutions were used to remove the residual Ni contaminants on poly-Si films. To obtain the optimized cleaning condition, various cleaning solutions [e.g., nitric acid treatment followed by oxide removal using hydrofluoric acid (HF) etching, and HCN cleaning] and cleaning parameters such as pH of the solutions (i.e., pH 10 and 11) and immersion times were optimized. The concentration of Ni contaminants on poly-Si films was estimated from total reflection X-ray fluorescence (TXRF) measurements. A 100 nm thick SiO_2 layer was then deposited as an insulator by PE-CVD at 250 °C. Fabrication of transistors with 20 μm width and 20 μm length was completed by deposition of 300 nm thick Mo electrodes using a sputtering method at room temperature. The electrical properties were evaluated with an Agilent 5270B parameter analyzer.

3. Results and Discussion

Fig. 1 shows the Ni concentration on the crystallized poly-Si surfaces determined from the TXRF spectra measured before (Fig. 1a) and after cleaning with various solutions for 10 min. The Ni concentration before cleaning was 4.5×10^{14} atoms/cm², and it was slightly decreased to 1.3×10^{14} atoms/cm² (Fig. 1b) and 1.1×10^{14} atoms/cm²

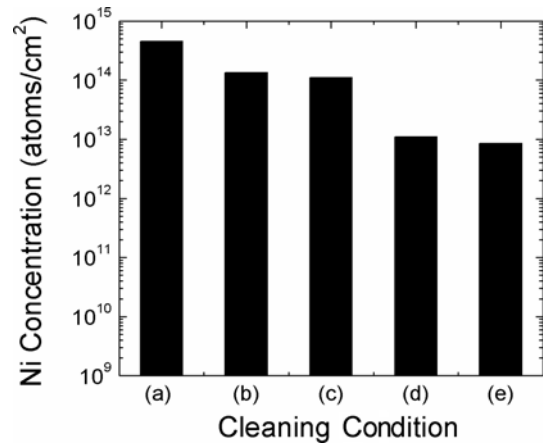


Fig. 1. Ni concentrations on the Ni-MILC poly-Si surfaces determined from the TXRF spectra measured before (a) and after cleaning for 10 min with following chemical solutions: (b) 0.027 % HCN aqueous solutions with pH 10, (c) 0.027 % HCN aqueous solutions with pH 11, (d) 68 wt% HNO_3 solutions, (e) 0.5 wt% HF solutions after the nitric acid treatment.

cm² (Fig. 1c) by cleaning using 0.027 wt% HCN aqueous solutions with pH 10 and 11, respectively. It has already been proved that Ni contaminants on Si surfaces can completely be removed by use of cyanide solutions.¹⁸⁾ The cleaning mechanism is associated with the formation of metal-cyanide complex ions by the reaction of CN^- ions in HCN solutions with metal species. The electro-dissociation probability of HCN increases with pH, resulting in an enhanced capability of metal removal with pH.¹³⁾ It implies that re-adsorption of Ni-cyanide complex ions, $[\text{Ni}(\text{CN})_2]^-$, $[\text{Ni}(\text{CN})_3]^{2-}$, and $[\text{Ni}(\text{CN})_4]^{3-}$, does not occur due to the weak formation energy between Ni-cyanide complex ions and Si, and high stability of these ions in aqueous solutions. Because of prevention of re-adsorption of Ni-cyanide complex ions, surface Ni species is effectively removed. Although the Ni concentration on the crystallized Si surface after HCN cleaning greatly decreased to $\sim 1/5$ that before cleaning, Ni was still present in the Si bulk because of Ni diffusion to the Si bulk during the Ni-MILC process.¹⁹⁾ When pH of HCN solutions is high, Si etching proceeds but that caused by pH 11 HCN solutions seems to be insignificant (etching rate for pH 11 HCN solutions: 2.5 nm/min).

The Ni concentration was markedly decreased to 1.1×10^{13} atoms/cm² by cleaning with 68 wt% HNO_3 aqueous solutions at room temperature (Fig. 1d). It is highly probable that Ni is accumulated in grain boundary regions, and the nitric acid treatment selectively etches away these regions. The Ni concentration was further decreased to 8.4×10^{12} atoms/cm² by etched-off of SiO_2 using 0.5 wt% HF solutions after the HNO_3 treatment (Fig. 1e). The nitric acid treatment forms a ~ 1.4 nm SiO_2

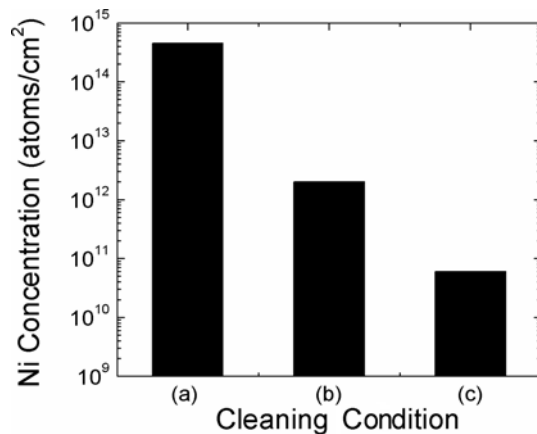


Fig. 2. Ni concentrations on the Ni-MILC poly-Si surfaces determined from the TXRF spectra: (a) before cleaning, (b) after cleaning with 0.027% HCN aqueous solutions of pH 10 for 2 min, (c) after that for 10 min.

layer,²⁰) and Ni contaminants included in the SiO₂ layer are removed by the subsequent HF etching.

The nitric acid oxidation and etching processes are difficult to avoid re-adsorption of Ni ions in the solutions unlike the HCN cleaning process.²¹) Therefore, we have employed the additional HCN cleaning process after the HF etching process, and the result is shown in Fig. 2. In the case of pH 10 HCN cleaning, Si etching can be neglected. Even in this case, the Ni concentration greatly decreased from 8.4×10^{12} atoms/cm² to 2.0×10^{12} atoms/cm². This decrease is attributable to removal of Ni re-adsorbed on the Si surface during the nitric acid treatment. When the time of cleaning using pH 10 HCN solutions was increased to 10 min, the Ni concentration further decreased to 6.0×10^{10} atoms/cm². This decrease is attributable to slight etch-off of the Si surface region by pH 10 HCN solutions.

Considering the above results, the most probable mechanisms of Ni removal are given below: Before cleaning, high concentration Ni is present on a poly-Si surface and grain boundary regions, and the concentration decrease with the depth (Fig. 3a). HCN solutions with pH of 10 remove Ni contaminants only on Si surfaces (Fig. 3b). HCN solutions with pH of 11 slightly etch away Si surface regions (Fig. 3c), and Ni in these regions is removed. However, Si etching proceeds relatively uniformly (i.e., the etching rate does not depend on the Ni concentration), resulting in the slight decrease in the Ni concentration. The nitric acid treatment, on the other hand, selectively etches away the grain boundary regions with high Ni concentrations (Fig. 3d), leading to a great decrease in the Ni concentration. We recently observed that the height of the ridge structure of poly-Si thin films produced by a laser annealing method with catalytic Ni

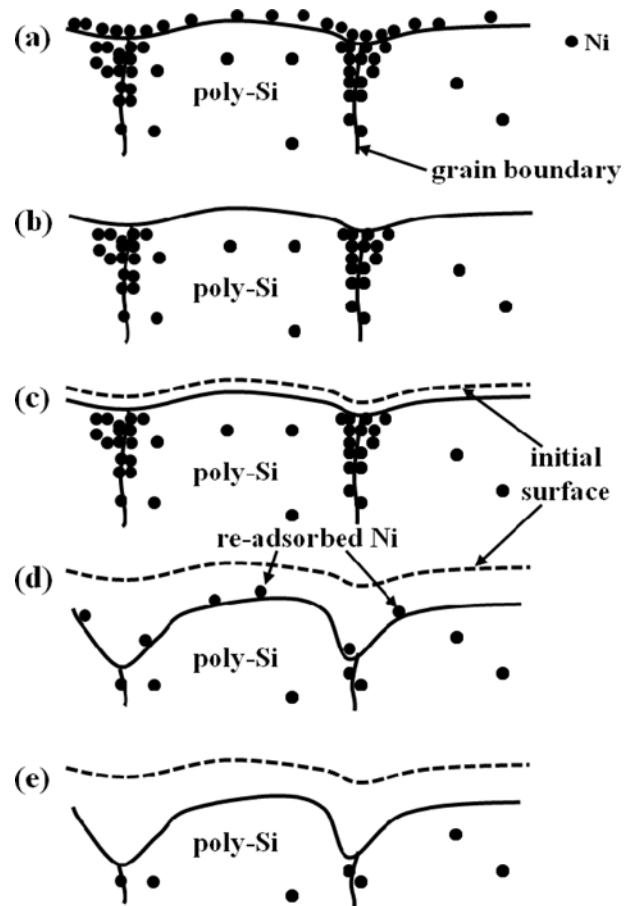


Fig. 3. Mechanisms of metal removal using the following methods: (a) before cleaning, (b) cleaning with pH 10 HCN solutions, (c) cleaning with pH 11 HCN solutions, (d) nitric acid treatment, (e) HF treatment followed by the nitric acid treatment.

greatly decreased by the nitric acid treatment, clearly showing that the treatment etched off grain boundary regions. (Grain boundaries are present at top regions of the ridge structure.) The nitric acid treatment forms a ~ 1.4 nm SiO₂ layer with the uniform thickness, and the SiO₂ removal does not considerably decrease the Ni concentration. During the nitric acid treatment, Ni ions in HNO₃ solutions are re-adsorbed on the Si surface. Re-adsorbed Ni can be removed by HCN cleaning (Fig. 3e).

Fig. 4 shows the SEM images for the poly-Si surfaces before and after the cleaning processes employed in Fig. 2. The crystallized Si surface without cleaning process did not show any features such as dendrite or island regions (Fig. 4a). Cleaning with pH 10 HCN solutions for 2 min showed minimal change in the surface morphology (Fig. 4b). On the other hand, etch pits were clearly observed on the Si surface cleaned with HCN solutions for 10 min (Fig. 4c). Ni-induced crystallization of amorphous Si is known to proceed with dendrite growth and defects are associated with the formation of dendrites.²²) The

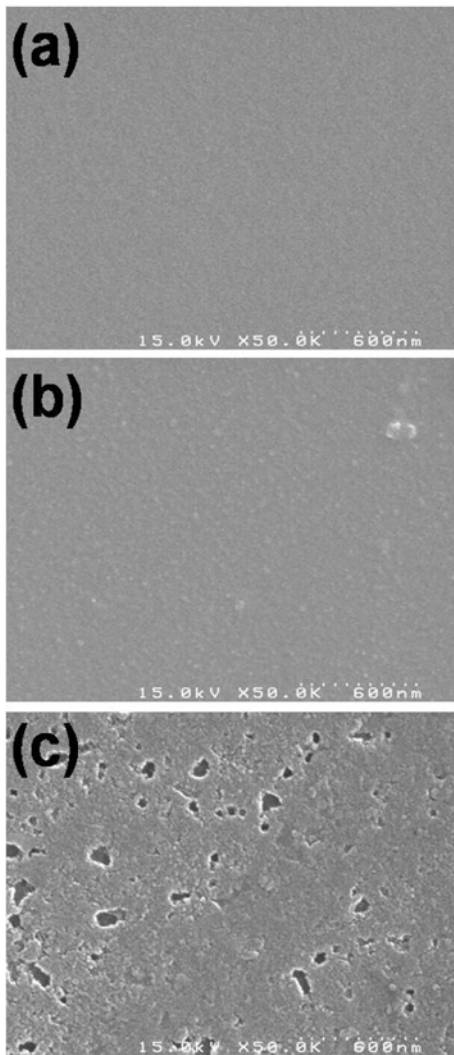


Fig. 4. SEM images of the Ni-MILC poly-Si surfaces: (a) before cleaning, (b) after cleaning with 0.027 % HCN aqueous solutions of pH 10 for 2 min, (c) after that for 10 min.

dendrite regions are relatively easy to be etched off by chemical solutions. Eventually, such a non-uniform surface of the HCN treated sample with etch pits is responsible for the increase in a leakage current density or performance failure of electronic devices. Considering these results, we selected the 2 min HCN cleaning condition followed by the nitric acid treatment plus the HF etching process.

In order to confirm the effect of removal of residual Ni contaminants in the Ni-MILC device, we prepared two different Ni-MILC poly-Si TFT samples and evaluated the electrical properties. One is the pristine sample and the other is the sample cleaned in the same way as that employed in Figs. 4(a) and (b). Fig. 5 shows the gate-voltage versus drain-current of the Ni-MILC poly-Si TFT devices at the drain bias of 0.1 V. Although the sample cleaned with HCN solutions for 2 min resulted in the

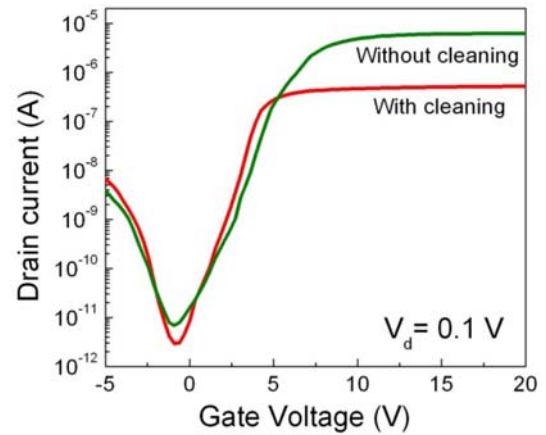


Fig. 5. Drain current vs. gate voltage curves of the poly-Si TFTs fabricated by Ni-MILC process: (a) without cleaning, (b) with cleaning using pH 10 HCN solutions for 2 min.

Table 1. Field effect mobility(μ_{FE}), threshold voltage(V_{th}), subthreshold swing(S.S), and off-state current density for the Ni-MILC with and without HCN cleaning process.

Type	Without cleaning	With cleaning
$\mu_{FE}(\text{cm}^2/\text{VS})$	75.5	95.5
$V_{th}(\text{V})$	4.9	3.1
S.S(V/dec)	1.37	0.65
Off-state current(A)	9.43×10^{-12}	3.43×10^{-12}

lower Ni concentration than that of the pristine sample, the surface of the cleaned sample was rougher than that of the pristine sample. The off-state current density, threshold voltage(V_{th}) and subthreshold swing(S.S) values of the TFTs depended on the cleaning processes. It turned out that those values before and after cleaning for 2 min were 9.4×10^{-12} A, 4.9 V, 1.33 V/dec and 3.4×10^{-12} A, 3.1 V, 0.65 V/dec, respectively. The detailed data are provided in Table 1. Ni atoms in Si act as deep-level trap sites. Elimination of Ni is likely to improve the device properties such as decreases in a leakage current density, S.S and V_{th} . It can be concluded that the lower off-state current, V_{th} and S.S values for the HCN-cleaned TFTs result from the effect of Ni removal.

4. Conclusion

We have developed the effective Ni cleaning method for Ni-MILC poly-Si TFTs and improved electrical properties of the TFTs. The HCN cleaning method alone slightly decreases the surface Ni concentration, but Ni in the Si bulk is not effectively removed. Using the nitric acid treatment, the Ni concentration decreases to almost two orders of magnitude lower than the initial concentration because the treatment etches away Si grain boundary

regions with a high Ni concentration. During the nitric acid treatment, some of Ni ions in the solution are likely to be re-adsorbed on the Si surfaces. Re-adsorbed Ni can effectively be removed by the HCN cleaning method. After HCN cleaning, the leakage current density, V_{th} and S.S values of the TFTs decrease from 9.4×10^{-12} A, 4.9 V, 1.33 V/dec to 3.4×10^{-12} A, 3.1 V and 0.65 V/dec, respectively.

References

1. M. Bonnel, N. Duhamel, L. Haji, B. Loisel and J. Stoemenos, *IEEE Electron Device Lett.*, **14**, 551 (1993).
2. S. Noguchi, S. Kiyama, S. Tsuda and S. Nakano, *Jpn. J. Appl. Phys.*, **32**, 6190 (1993).
3. K. Shimizu, O. Sugiura and M. Matsumura, *IEEE Trans. Electron Devices*, **40**, 112 (1993).
4. R. Bachrach, K. Winer, J. Boyce, S. Ready, R. Johnson and G. Anderson, *J. Electron. Mater.*, **19**, 241 (1990).
5. G. Giust and T. Sigmon, *IEEE Trans. Electron Devices*, **45**, 925 (1998).
6. D. Fork, G. Anderson, J. Boyce, R. Johnson and P. Mei, *Appl. Phys. Lett.*, **68**, 2138 (1996).
7. R. Cammarata, C. Thompson, C. Hayzelden and K. Tu, *J. Mater. Res.*, **5**, 2133 (1990).
8. O. Nast and A. J. Hartmann, *J. Appl. Phys.*, **88**, 716 (2000).
9. J. B. Lee, C. J. Lee and D. K. Choi, *Jpn. J. Appl. Phys.*, **40**, 6177 (2001).
10. D. Murley, N. Young, M. Trainor and D. McCulloch, *IEEE Trans. Electron Devices*, **48**, 1145 (2001).
11. H. Kobayashi, Y. L. Liu, Y. Yamashita, J. Ivánčo, S. Imai and M. Takahashi, *Sol. Energy*, **80**, 645 (2006).
12. N. Fujiwara, Y. L. Liu, M. Takahashi and H. Kobayashi, *J. Electrochem. Soc.*, **153**, G394 (2006).
13. M. Takahashi, Y. L. Liu, N. Fujiwara, H. Iwasa and H. Kobayashi, *Solid State Commun.*, **137**, 263 (2006).
14. M. Madani, Y. L. Liu, M. Takahashi, H. Iwasa and H. Kobayashi, *J. Electrochem. Soc.*, **155**, H895 (2008).
15. O. Maida, A. Asano, M. Takahashi, H. Iwasa and H. Kobayashi, *Surf. Sci.*, **542**, 244 (2003).
16. D. R. Lide, *CRC Handbook of Chemistry and Physics*, 75th ed., p.951, CRC Press, Inc., Boca Raton, USA (1995).
17. K. Cheng, J. Lee and J.W. Lyding, *Appl. Phys. Lett.*, **77**, 3388 (2000).
18. N. Fujiwara, Y. L. Li, T. Nakamura, O. Maida, M. Takahashi and H. Kobayashi, *Appl. Surf. Sci.*, **235**, 372 (2004).
19. Z. Jin, K. Moulding, H.S. Kwok and M. Wong, *IEEE Trans. Electron Devices*, **46**, 78 (1999).
20. W. B. Kim, T. Matsumoto and H. Kobayashi, *Appl. Phys. Lett.*, **93**, 072101 (2008).
21. J. Ryuta, T. Yoshimi, H. Kondo, H. Okuda and Y. Shimanuki, *Jpn. J. Appl. Phys.*, **31**, 2338 (1992).
22. F. Edelman, C. Cytermann, R. Brener, M. Eizenberg, Y. L. Khait, R. Weil and W. Beyer, *J. Appl. Phys.*, **75**, 7875 (1994).